Solid State Communications 252 (2017) 1–5

Contents lists available at ScienceDirect

Solid State Communications

journal homepage: www.elsevier.com/locate/ssc

Communication

Electronic and magnetic properties of TM atoms adsorption on 2D silicon carbide by first-principles calculations

M. Luo[a,*], Y.H. Shen[b], T.L. Yin[b,c]

[a] Department of Electronic Engineering, Shang Hai Jian Qiao University, Shanghai 201306, P.R. China
[b] Key Laboratory of Polar Materials and Devices, East China Normal University, Shanghai 200241, P.R. China
[c] School of Electronics and Information, Nantong University, Nantong 226019, P.R. China

ARTICLE INFO

Keywords:
SiC monolayer
TM adsorption
DFT
Magnetic properties

ABSTRACT

The magnetic properties of different transition-metal (TM) atoms (TM=Co, Cu, Mn, Fe, and Ni) adsorption on SiC monolayer are investigated using density functional theory (DFT). Magnetism appears in the cases of Co, Cu, Mn, and Fe. Among all the magnetic cases, the Co-adsorbed system has the most stable structure. Therefore, we further study the interaction in the two-Co-adsorbed system. Our results show that the interaction between two Co atoms is always FM and the *p–d* hybridization mechanism results in such ferromagnetic states. However, the FM interaction is obviously depressed by the increasing Co-Co distance, which could be well explained by the Zener-RKKY theory. Moreover, different magnetic behavior is observed in the two-Mn-adsorbed system and a long-range AFM state is showing. Such multiple magnetic properties may suggest promising applications of TM-adsorbed SiC monolayer in the future.

1. Introduction

Silicon carbide (SiC) has attracted much interest due to its corrosion resistance, large band gap, high mechanical strength, low density, high hardness, high thermal conductivity and low thermal expansion coefficient [1–5]. Similar to graphene, the SiC monolayer (2D-SiC) with a honeycomb structure could be energetically stable [6,7] and SiC monolayer exhibits a large direct band gap [8]. Several theoretical studies investigated the structure and electronic properties of SiC nano scales [9,10]. Due to its wide band gap (3.2 eV), SiC has potential applications in electronics and optics. Recently a large number of researchers have given special attention to the properties of metal doped 2D materials [11–14] and high catalytic activity has been verified. Recently, atoms adsorption on 2D nanosheet also has been studied [15–17]. In particular, Naji et al. [18] and Yagi et al. [19] have investigated the magnetic properties of transition-metal (TM) atoms adsorption on graphene by the first principles calculations, respectively. Different magnetic behavior has been found in TM-adsorbed graphene and those results could be useful for spintronics applications. In order to find its potential applications, we study TM atoms adsorption on SiC monolayer by using the same method.

In this work, the magnetic properties of SiC monolayer with different TM atoms and adsorption sites are investigated using first-principles method. Magnetism is observed in the cases of Co, Cu, Mn, and Fe. Among all the magnetic cases, the Co-adsorbed system shows a most stable structure. Therefore, the interaction between two Co atoms adsorption on SiC monolayer is further studied. The results show the *p–d* hybridization mechanism between Co and its neighboring C and Si atoms induces its ferromagnetic (FM) state. Moreover, different magnetic behavior appears in the two-Mn-adsorbed system and a long-range antiferromagnetic (AFM) coupling is observed. Such multiple magnetic properties might be suitable for applications in electronics and spintronics.

2. Method

Our calculations are performed first-principles method based on density functional theory (DFT) within the generalized gradient approximations (GGA-PBE) [20] as implemented in the VASP package [21]. The projector augmented-wave (PAW) [22] pseudopotential method is used and the cut-off energy is 500 eV. The 4×4×2 k-points were used in both 5×5×1 and 8×5×1 supercells. The lattice parameter and bond length of SiC monolayer is 3.094 and 1.786 Å [23], respectively. The separation between two layers is 20 Å. All the calculations are self-consistent and the total energy convergence criterion is set at the value of 10^{-5} eV.

* Correspondence to: Department of Electronic Engineering, ShangHai Jian Qiao University, NO.1111, Huchenghuan Road, Pudong New District, Shanghai, China
E-mail address: mluo@gench.edu.cn (M. Luo).

http://dx.doi.org/10.1016/j.ssc.2017.01.003
Received 8 September 2016; Received in revised form 25 December 2016; Accepted 7 January 2017
Available online 09 January 2017
0038-1098/

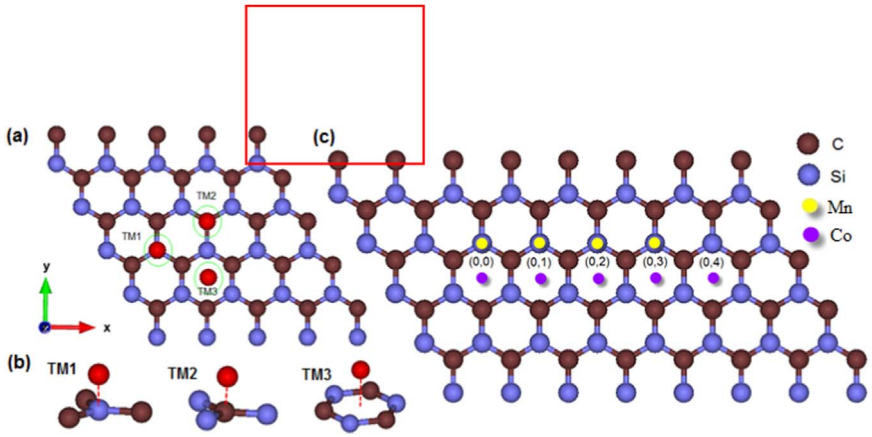

Fig. 1. (Color online) (a) Top view of three different adsorption sites in the 5×5×1 SiC monolayer marking as TM1, TM2 and TM3, respectively; (b) side view of the adsorption sites; (c) the configurations of two Mn (Co) atoms adsorption on the 8×5×1 SiC monolayer.

3. Results and discussions

3.1. Electronic structures and magnetism of TM-adsorbed SiC monolayer

Firstly, we study the magnetic properties of several TM (TM=Co, Cu, Mn, Fe, and Ni) atoms adsorption on SiC monolayer. There are three possible adsorption sites on the SiC monolayer. As shown in Fig. 1(b), the TM atom may combine with the Si atom, or bond with the C atom, or locate in the center of the hexagon, which is labeled as TM1, TM2 and TM3, respectively. The total magnetic moments (μ_{total}), adsorption energy and bonding length are listed in Table 1. Here, the adsorption energy is estimated as $E_{ads}=E_T-E_P-E_{TM}$, where E_P and E_T is the total energy of SiC monolayer with no defects and with a TM dopant, respectively; E_{TM} is the energy of a TM atom. According to the calculated adsorption energies, the stable adsorption sites of the five TM atoms are quite different. For Co and Fe atoms, the most favorable site is TM3 and the value of adsorption energy is −2.432 and −1.949 eV, respectively. The most favorable site of Cu and Ni atoms is TM2 and the calculated adsorption energy is −0.858 and 2.826 eV. But for the Mn atom, the most favorable site is TM1 and the value is −2.270 eV. Moreover, magnetic behavior appears in the cases of Cu, Co, Fe, and Mn, and the values of μ_{total} are 0.9984, 0.9996, 1.9997, and 4.9999 μB, respectively. Nonmagnetic states are observed in the Ni-adsorbed SiC monolayer.

Next, we analyze the electronic properties of TM-adsorbed SiC monolayer. Their densities of states (DOS and PDOS) are shown in Fig. 2. For Co-, Cu-, Mn-, and Fe-adsorbed systems, seen in Fig. 2(a)-(d), there are some splitting energy levels around the Fermi level (E_F), which arise from the hybridization between the TM (TM=Co, Cu, Mn, and Fe) dopant and its neighboring Si and C atoms. Hence, the systems exhibit magnetic behavior. As shown in Fig. 2(e), there is no splitting energy level around the E_F. That is why it is nonmagnetic. Similar trends have been found in the previous studies [17,18]. Moreover, as listed in Table 1, the magnetic moments of five dopants are different. The total magnetic moments of Mn-, Fe-, Co-, Cu-, and Ni-doped systems are 4.9999, 1.9997, 0.9996, 0.9984, and 0.0 μ_B, respectively. The local magnetic moment is about 3.953, 1.556, 0.714, and 0.722 μ_B on Mn, Fe, Co, and Cu atoms, respectively. As we know, the induced local magnetic moment can be made due to the different populations of TM atomic *3d* orbit after its hybridization with C and Si atoms in our cases. For up spin state of the Mn (Cu) atom we have a $3d^{4.879}(3d^{1.279})$ population while the down spin state has a population as $3d^{0.926}$ $(3d^{0.557})$. For down spin state of the Fe (Co) atom, we have a $3d^{2.422}$ $(3d^{1.375})$ population while the up spin state has a population as $3d^{0.866}$ $(3d^{0.661})$. Obviously, the net 3d populations of Mn, Fe, Co, and Cu atoms are different, then different magnetic moments are shown in these four systems. In addition, for the Ni-doped system, the population of up spin and down spin states are equal to each other, thus the net population is zero and no magnetism is expected.

Table 1
Adsorption energy (E_{ads}), total magnetic moment (μ_{total}) and TM-C and TM-Si bond lengths (L) in the TM-adsorbed 5×5×1 SiC monolayer. (♦) denotes the most stable structure.

Structure		Co	Cu	Fe	Mn	Ni
E_{ads} (eV)	TM1	−1.163	−0.568	−1.134	−2.270♦	−2.501
	TM2	−2.423	−0.858♦	−1.827	-2.066	−2.826♦
	TM3	−2.432♦	−0.734	−1.949♦	−1.997	−2.617
μ_{total} (μ_B)	TM1	3.0003	0.9984	3.9998	4.9999♦	0.0
	TM2	0.9998	0.9999♦	1.9998	2.9998	0.0
	TM3	0.9996♦	0.9993	1.9997♦	2.9999	0.0
L♦ (Å)	TM-Si	2.278	2.434	2.313	2.431	1.906
	TM-C	2.256	2.110	2.297	2.179	2.406

3.2. Magnetic coupling in Co-adsorbed SiC monolayer

As shown in Table 1, among four magnetic systems, the Co-adsorbed system has the lowest adsorption energy of −2.432 eV, which indicates the system is the most stable. Because of this, we come to investigate the interaction in this system of 8×5×1 supercell, and several possible configurations of Co dopants are shown in Fig. 1(c). We use i to mark the dopant Co (0, i) and one Co atom is fixed [denoted 0 in Fig. 1(c)], and another adsorbed Co dopant is marked as i=1–3. From our calculations, the ferromagnetic coupling depends on Co-Co distance, as listed in Table 2. In addition, the stability of FM states is determined by total energy difference ($\Delta E=E_{AFM}-E_{FM}$) between the antiferromagnetic (AFM) and ferromagnetic (FM) states for each configuration.

For the two-Co-adsorbed system, ΔE changes from 297 to 2 meV with increasing Co-Co distance, which means that the magnetic coupling between two Co dopants is always FM. To explain the FM interaction, the TDOS and PDOS for the nearest two Co atoms are plotted in Fig. 3. From Fig. 3(b)–(e), there is an obvious *p-d* hybridization exhibiting in Co and its adjacent Si/C atoms. Due to the *p-d* hybridization, the minority spin states are lifted upward together with the downward shift of the majority spin states, which lead to the total energy of the system lowering [24]. Thus, the *p-d* hybridization leads to the FM interaction in two-Co-adsorbed SiC monolayer. Moreover, the total magnetic moment is 2.00 μ_B. As we know, the different local distortions lead to different spin distributions of the magnetic moment. As illustrated in Fig. 4, the main spin charge densities are distributed on two Co dopants. The interaction between a

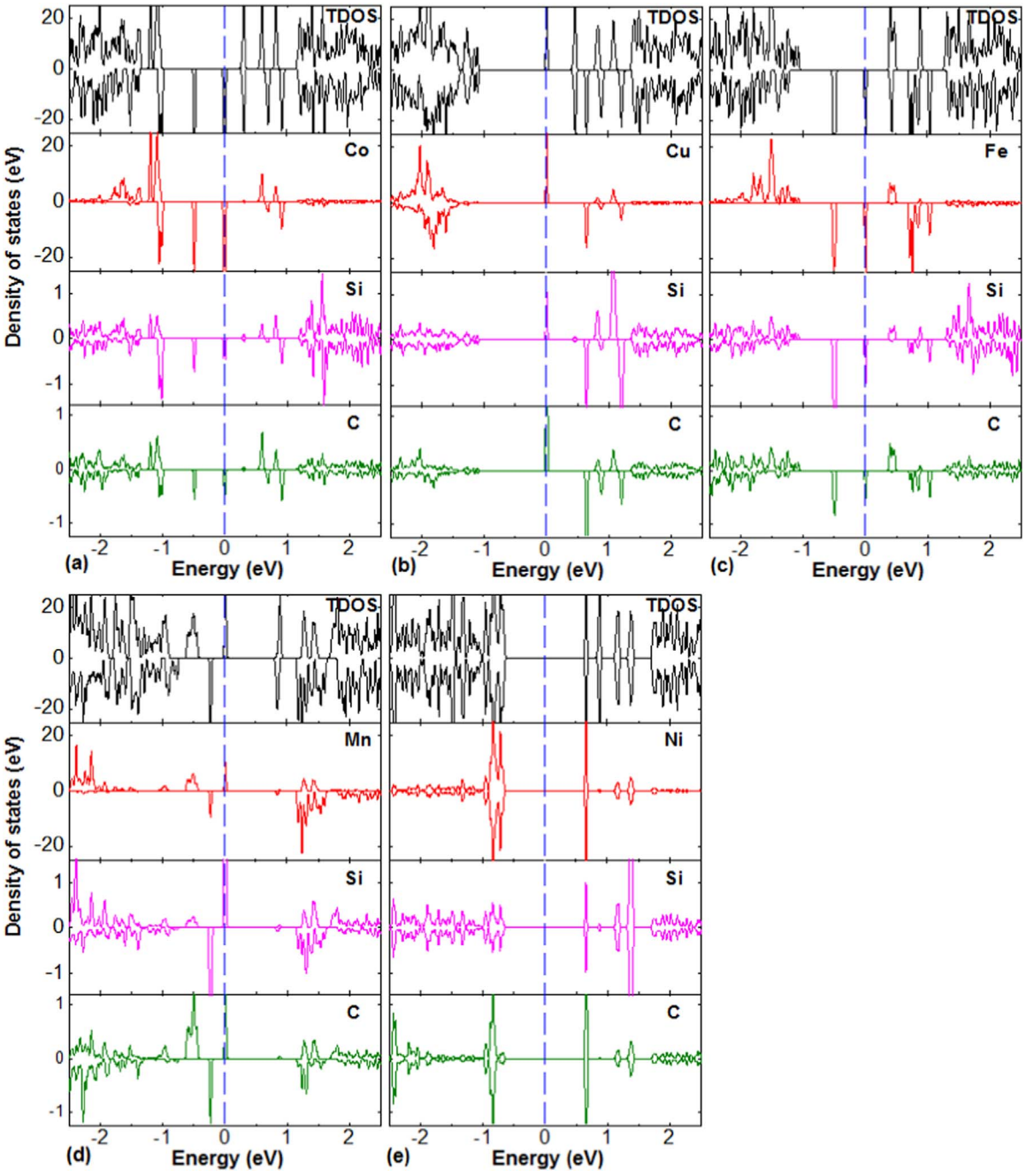

Fig. 2. (Color online) Spin-polarized DOS and PDOS of TM-adsorbed SiC monolayer of 5×5×1 supercell (TM denotes Co–Ni). The Fermi level is marked by blue dashed line.

Table 2
Optimized TM-TM distance ($d_{TM\text{-}TM}$), total magnetic moments (M_{tot}), total energies (E_{tot}), energy differences between AFM and FM (ΔE) and the configurations of TM atoms are as shown in Fig. 1(c).

Structure	Configuration	$d_{TM\text{-}TM}$ (Å)	M_{tot} (μ_B)	E_{tot} (eV)	ΔE (eV)
$Si_{40}Co_2C_{40}$	1	2.995	2.00	−572.604	0.297
	2	6.205	2.00	−571.803	0.034
	3	9.297	2.00	−571.770	0.002
$Si_{40}Mn_2C_{40}$	1	3.106	–	−575.516	−0.144
	2	6.187	–	−575.342	−0.012
	3	9.296	–	−575.351	−0.002

Co dopant and its adjacent Si/C atoms is antiferromagnetic, which exhibits a p character of the spin-polarized states of Si and C atoms. Therefore, the total magnetic moment (2.00 μ_B) mainly arises from the polarization of two Co *d* states (1.733 μ_B) and their nearest-neighboring S/C *p* states (0.198 μ_B).

It is noteworthy that a much larger Co-Co distance [12.443 Å, case (0,4) in Fig. 1(c)] is further considered and the ΔE is extremely small (~1 meV). This result indicates that the FM interaction under such conditions is very weak. The FM interaction between two Co dopants is evidently depressed by the increasing Co-Co distance. Therefore, to describe the special magnetic behavior in Co/SiC system properly, we parameterized the exchange interactions between Co dopants using a simple Heisenberg model [25]. The exchange interaction coefficient $J(r)$ is parameterized using the functional form

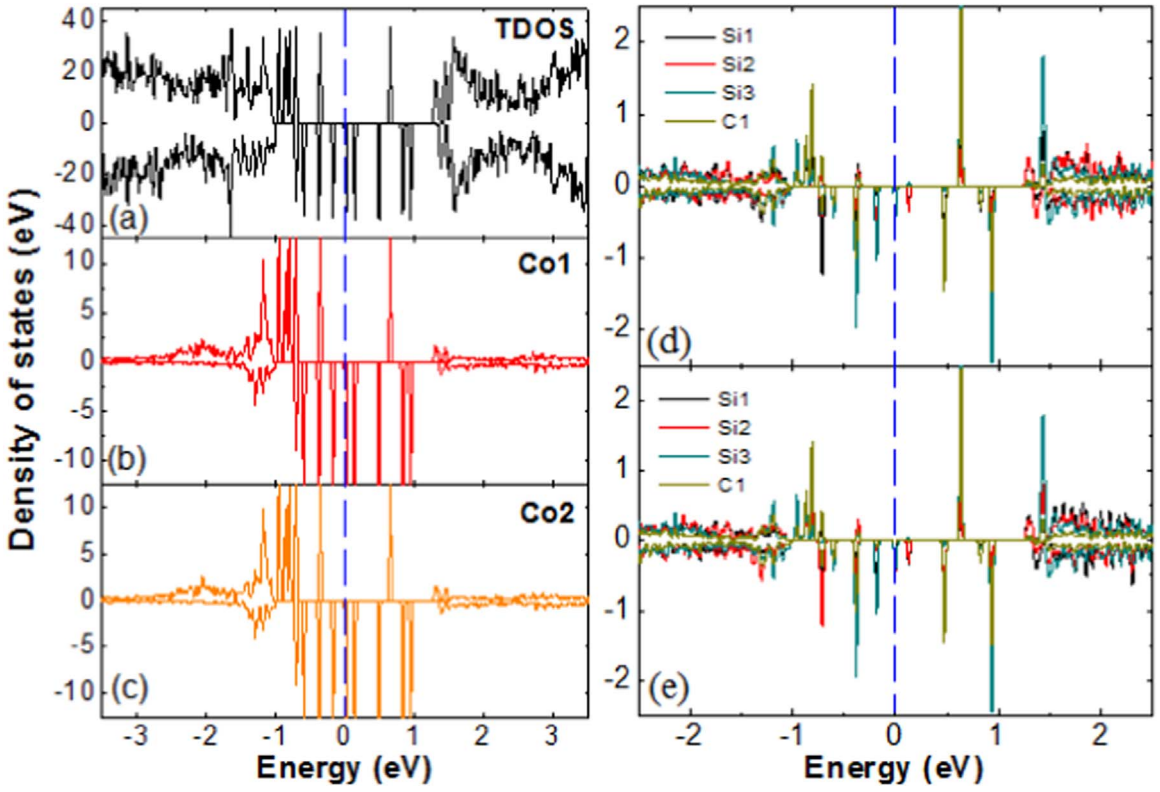

Fig. 3. (Color online) (a) DOS for two-Co-adsorbed 8×5×1 SiC monolayer ; (b) and (c) PDOS for two Co atoms, and (d) and (e) its adjacent C and Si atoms, respectively.

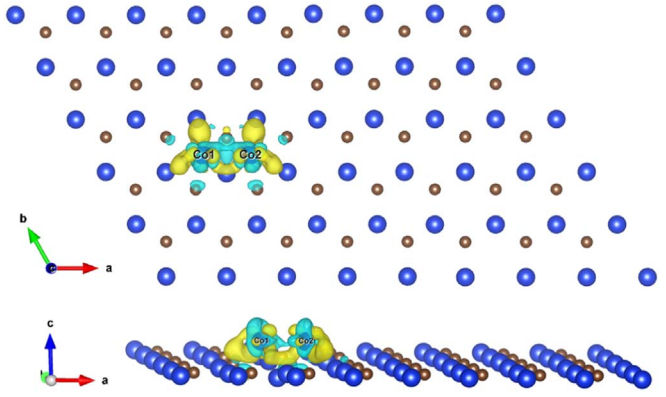

Fig. 4. (Color online) Calculated spin density distribution in Co-adsorbed SiC monolayer of 8×5×1 supercell. Yellow and cyan isosurfaces represent positive and negative spin densities (0.008 e/Å^3), respectively.

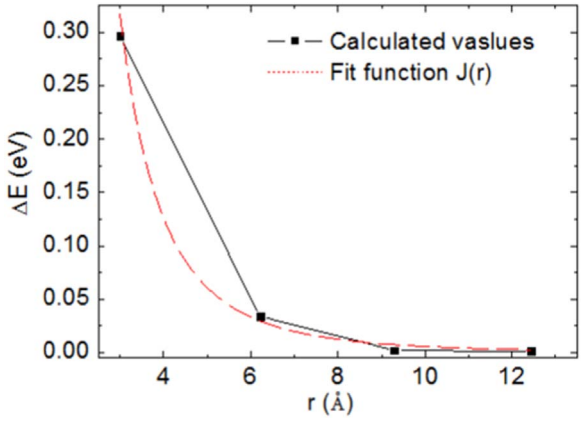

Fig. 5. The total energy difference (ΔE) as a function of the Co-Co distance (r). The dashed line is the Magnetic correlation function [J(r)] vs the Co-Co distance (r).

$$J(r) = \begin{cases} \frac{c}{r^3}\exp(-r/r_0) & r \le r_c \\ 0 & otherwise \end{cases} \quad (1)$$

where r is the distance between two Co atoms, r_0 is the screening length, r_c is the cutoff in the interaction range depending on the radius of the fifth nearest-neighbor shell, and c is a constant of proportionality [26]. The cutoff length is taken as r_c=15.39 Å. The coefficients c and r_0 are obtained by fitting the energy differences $\Delta E = E_{AFM} - E_{FM}$ and the fitting parameters are c=10.15 eV/Å^3 and r_0=17.15 Å. We simulate the magnetic correlation function $J(r)$ to the Co-Co distance (r), as shown in Fig. 5. The simulation describes the trend between the calculated energy difference (ΔE) and the Co-Co distance (r) reasonably. As we know, the long range FM interaction between TM dopants while the hybridization is weak which can be well explained by the Zener-RKKY theory [27].

Finally, due to the high adsorption energy (−2.270 eV) and the largest magnetic moment (4.9999 μ_B), we also investigate the interaction in two-Mn-adsorbed SiC monolayer and the possible configurations of Mn dopants are shown in Fig. 1(c) as well. However, quite different magnetic behavior is found. As shown in Table 2, ΔE changes from −144 to −2 meV with increasing Mn-Mn distance, which indicates an AFM coupling between two Mn atoms. Similarly, the AFM coupling has been evidently depressed by the increasing Mn-Mn distance. The PDOS of the nearest two-Mn-adsorbed system is plotted in Fig. 6. From Fig. 6(b)–(e), there are some hybrids around E_F, which come from two Mn atoms and their adjacent Si/C atoms. The hybridization of one energetically localized below and the other one well above E_F. Hence, the system shows null spin polarization, as shown in Fig. 6(a). Furthermore, the E_F approaches the upper band. In this situation, the superexchange takes over, destroying the ferromagnetism [26]. Thus, the preferred magnetic coupling between two Mn atoms should be AFM with null spin polarization. Moreover, the superexchange represents a rather strong interaction for wide-gap semiconductors,

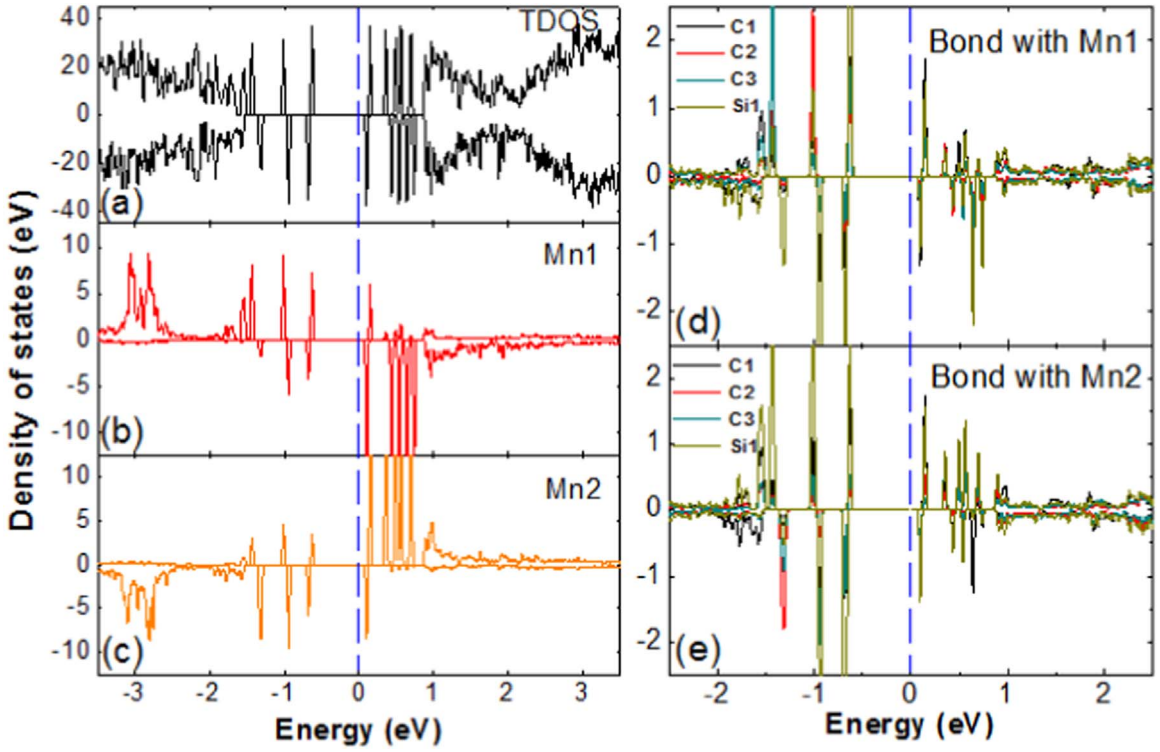

Fig. 6. (Color online) (a) DOS for two-Mn-adsorbed SiC monolayer in the 8×5×1 supercell; (b) and (c) PDOS for two Mn atoms, respectively; (d) and (e) their adjacent Si and C atoms, respectively.

where the interaction is very short ranged. Therefore, as the Mn-Mn distance increases, the AFM coupling has been seriously reduced. Such distinct magnetic properties render the TM-adsorbed SiC monolayer a valuable material. More detailed studies need to be done in the future.

4. Conclusions

Based on density function theory, we have systemically studied the magnetic properties of SiC monolayer adsorbed with series TM (TM=Co, Cu, Mn, Fe, and Ni) atoms. The magnetic states are observed in the cases of Co, Cu, Mn, and Fe. From our calculations, the Co-adsorbed SiC monolayer is the most stable system. Then, the FM coupling in the two-Co-doped system is studied. Our results show that the ferromagnetic states are originated by the p–d hybridization between Co and its adjacent Si/C atoms. However, the FM interaction was obviously depressed with increasing Co-Co distance, which could be explained by the Zener-RKKY theory. Moreover, we also investigated the interaction in the two-Mn-adsorbed system and a decaying AFM interaction is observed.

Acknowledgments

The work is supported by the Shanghai Committee of Science and Technology, China (Grant No. ZHT. K1507). We also thank the Supercomputer Center of ECNU for using the Dawn 5000A supercomputer.

References

[1] P.A. Ivanov, V.E. Chelnokov, Semicond. Sci. Tech. 7 (1992) 863–880.
[2] T. Narushima, T. Goto, T. Hirai, Y. Iguchi, Mater. Trans. JIM 38 (1997) 821–835.
[3] S.Z. Wang, L.Y. Xu, B.Y. Shu, B. Xiao, J.Y. Zhuang, E.W. Shi, J. Inorg. Mater. 14 (1999) 527–534.
[4] J.B. Casady, R.W. Johnson, Solid-State Electron. 39 (1996) 1409–1422.
[5] K. Watari, J. Ceram. Soc. Jpn. 109 (2001) S7–S16.
[6] F. Claeyssens, C.L. Freeman, N.L. Allan, Y. Sun, M.N.R. Ashfolda, J.H. Harding, J. Mater. Chem. 15 (2005) 139–148.
[7] C.L. Freeman, F. Claeyssens, N.L. Allan, Phys. Rev. Lett. 96 (2006) 066102–066105.
[8] H.C. Hsueh, G.Y. Guo, S.G. Louie, Phys. Rev. B 84 (2011) (085404-085413).
[9] M.B. Javan, J. Magn. Magn. Mater. 401 (2016) 656–661.
[10] N. Alaal, V. Loganathan, N. Medhekar, A. Shukla, J. Phys. D: Appl. Phys. 49 (2016) 105306–105314.
[11] Y.C. Cheng, Z.Y. Zhu, W.B. Mi, Z.B. Guo, U. Schwingenschlögl, Phys. Rev. B 87 (2013) 100401–100404.
[12] M. Luo, Y.H. Shen, T.L. Yin, AIP Adv. 6 (2016) 085112.
[13] B. Huang, H. Xiang, J. Yu, S.H. Wei, Phys. Rev. Lett. 108 (2012) 206802–206805.
[14] X. Zhao, C.X. Xia, T.X. Wang, X.Q. Dai, Soild State Commun. 220 (2015) 31–35.
[15] H. Yildirim, A. Kinaci, Z.J. Zhao, Maria K.Y. Chan, J.P. Greeley, ACS Appl. Mater. Interfaces 6 (2014) 21141–21150.
[16] G.S. Grigorkina, I.V. Tvauri, A.G. Kaloeva, O.G. Burdzieva, D. Sekiba, S. Ogura, K. Fukutani, T.T. Magkoev, Sold. State Commun. 233 (2016) 11–14.
[17] B. Zhao, C.Y. Li, L.L. Liu, B. Zhou, Q.K. Zhang, Z.Q. Chen, Z. Tang, Appl. Surf. Sci. 382 (2016) 280–287.
[18] S. Naji, A. Belhaj, H. Labrim, M. Bhihi, A. Benyoussef, A. El Kenz, J. Phys. Chem. C 118 (2014) 4924–4929.
[19] Y. Yagi, T.M. Briere, M.H.F. Sluiter, V. Kumar, A.A. Farajian, Y. Kawazoe, Phys. Rev. B 69 (2004) (075414-075422).
[20] J.P. Perdew, K. Burke, M. Ernzerhof, Phys. Rev. Lett. 77 (1996) (3865-3858).
[21] G. Kresse, J. Furthmüller, Phys. Rev. B 54 (1996) 11169–11186.
[22] G. Kresse, D. Joubert, Phys. Rev. B 59 (1999) 1758–1775.
[23] S.S. Lin, J. Phys. Chem. C 116 (2012) 3951–3955.
[24] C. Zener, Phys. Rev. 81 (1951) 440–444.
[25] A. Ramasubramaniam, D. Naveh, Phys. Rev. B 87 (2013) 195201.
[26] K. Sato, L. Bergqvist, J. Kudrnovský, P.H. Dederichs, O. Eriksson, I. Turek, B. Sanyal, G. Bouzerar, H. Katayama-Yoshida, V.A. Dinh, T. Fukushima, H. Kizaki, R. Zeller, Rev. Mod. Phys. 82 (2010) 1633–1690.
[27] J. Kanamori, K. Terakura, J. Phys. Soc. Jpn. 70 (2001) 1433–1434.